

# Study on Microstructure and Properties of the Additive Layer of FCW Wire for H13 Steel

Xinhua Xiao\*

University Science Park, Hubei Institute of Technology University Science and Technology, Huangshi 435003, Hubei, China

\*Corresponding author, E-mail: [xiaoxinhua12@126.com](mailto:xiaoxinhua12@126.com)

## Abstract:

*In order to provide research data on direct forming and rapid recovery of metal parts by arc fuse additive manufacturing technology. In this paper, the flux cored wire prepared from H13 die steel strip was used as the wire material, and the arc additive manufacturing process was used to carry out multi-channel and multi-layer surfacing welding process test on the Cr12MoV steel substrate, and the quality, structure and performance of the additive layer were studied. The results show that there is obvious fusion line between layers, and there is no porosity, crack or unfusion in the section. The average interlayer microhardness was 325HV, slightly higher than that of annealed substrate. The change pattern of microstructure from bottom to top layer is from equiaxed crystal to larger equiaxed crystal. The top layer is columnar crystal, and the microstructure is mixed structure of martensite, alloy compound and bainite. The tensile test showed that the tensile strength between layers was about 700Mpa, with no obvious yield strength and the elongation reaching 11.9%. The wear test shows that the additive layer has better wear resistance, and wear is a mixture mechanism of abrasive wear and adhesive wear. H13 steel flux-cored wire is suitable for direct manufacture of wear - resistant parts and mold repair.*

## Keywords:

*Arc fuse additive manufacturing, Mold repair, Mechanical properties, Friction and wear*

## 1 Introduction

In the mould manufacturing industry, moulds are subjected to large stresses and deformations due to their alternating harsh service environments, which ultimately lead to wear and tear, cracks, fractures, and eventual failure. Technological innovation has led to the study of mould remanufacturing technology, and currently, the commonly used repair technologies include thermal spraying, laser cladding technology, electric spark, electric arc surfacing (arc additive manufacturing), and electrobrush plating, etc [1-5]. Among them, arc wire additive manufacturing (WAAM) technology is one of the important research directions in the field of 3D additive manufacturing of metal materials, and the research boom of direct forming metal parts and parts repair by arc wire additive manufacturing technology is being set off at home and abroad. For this reason, this paper selects H13 mould steel with coated alloy powder prepared flux-cored wire as wire material, using arc additive manufacturing technology, multi-channel multi-layer 3D overlay welding of straight-walled parts on the mould steel substrate, to carry out research on the organisation and properties of the mould steel arc additive layer, to provide data support for the development of processes and materials for the remanufacturing of moulds and the direct manufacturing of parts and other aspects.



© 2025 by the author(s); licensee Mason Publish Group, this work for open access publication is under the Creative Commons Attribution International License (CC BY 4.0). (<http://creativecommons.org/licenses/by/4.0/>)

## 2 Testing and Analysis

### 2.1 Research on multi-layer and multi-pass forming process

In the test with the use of argon as a shielding gas, gas flow rate of 16L/min, welding speed of 5mm/s, the distance from the nozzle to the workpiece is 10.5mm, the current is 110A, the voltage is 20V, the flux-cored wire prepared from H13 mould steel strip is used as the wire material, and the arc additive manufacturing technology is used to carry out multi-layer overlays on the Cr12MoV mould steel substrate, and the temperature of the interlayer is controlled at 150 ~ 200°C. Round-trip 4-channel 15-layer high multi-channel multilayer cladding layer, will be obtained after 15 layers of size of about 120mm × 50mm × 8mm arc 3D additive material multichannel multilayer vertical wall pieces cut corrosion and polishing, the macroscopic organisation of the photographs obtained as shown in Figure 1: Observation of Figure 1 shows that there are obvious boundaries between the layer and the layer, the thickness of the layer between the fluctuations in the 2.1 ~ 2.3mm, from the macroscopic morphology of the cross-sectional observation of the absence of porosity No air holes, cracks, no unfused and other phenomena, indicating that the arc 3D additive interlayer bonding is good, dense organisation; the measured composition of the molten metal is shown in Table 1.

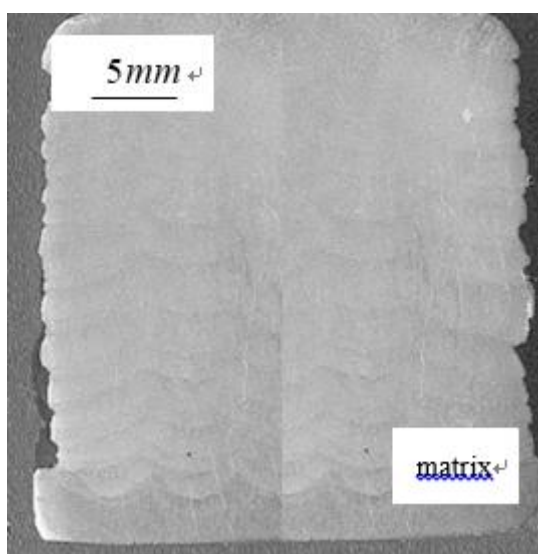


Figure 1: Macroscopic morphology of additive layer

Table 1 Composition of deposited metal (mass percentage) %

C	Ni	Cr	Mo	V	Si	Mn	P	S	%
0.2	1.5	1.9	0.9	0.5	0.3	1.1	≤0.	≤0.	
1~0	~1.	~3.	~1.	1~0	1~0	1~1	03	03	
.32	7	1	1	.59	.38	.21			

### 2.2 Hardness and mechanical properties

#### 2.2.1 Hardness Test

Hardness is an index of the comprehensive mechanical properties of materials. For this reason, the Vickers microhardness test was carried out on the additive layer specimen, and the test results are shown in Figure 2. It can be seen that the average hardness of the arc 3D additive layer of 325HV, in which the hardness value of

the lower part of the vertical wall pieces is slightly lower than the upper part of the hardness value, this is due to the lower layer of the substrate is close to the bottom of the bottom layer of heat dissipation conditions are better than the upper layer of the metal, the microstructure is dense, the compound hard phase is not anxious to gather, the distribution of hardness value is more uniform; the higher the hardness value of the additive is the more on the higher side, this is due to the latter layer of the accumulation of heat, the more carbides gathered grain boundaries, resulting in stress concentration hardness is high. This is due to the accumulation of heat in the latter layer, more carbides gathered at grain boundaries, resulting in high stress concentration hardness. The hardness of the entire additive layer is higher than the substrate (annealed cold work mould steel Cr12MoV microhardness of 310 ~ 257HV), it can be seen, the additive layer of comprehensive mechanical properties.

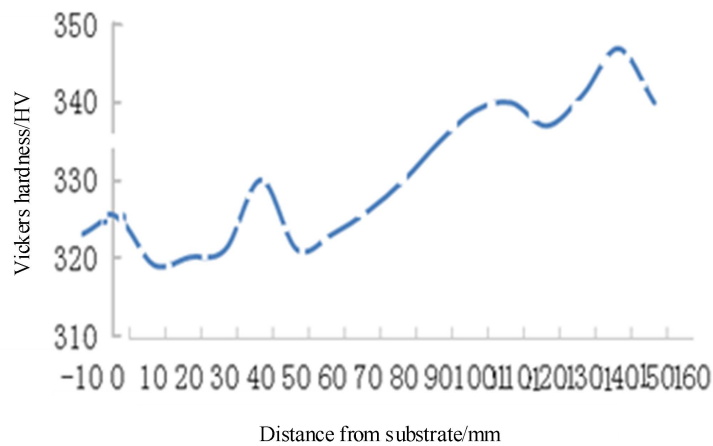


Figure 2: Hardness distribution from the substrate towards the additive layer in the height direction

### 2.2.2 Tensile test

Use WDW-100 type universal testing machine arc 3D additive material after the addition of single-pass multilayer vertical wall piece specimens for room temperature tensile performance testing, determination of its strength index. According to GB/T 228-2002 'room temperature tensile test methods for metal materials' and GB/T 2652-2008 'weld and molten metal tensile test methods' standard, multi-channel multilayer specimens for wire cutting to produce tensile specimens, tensile specimen size as shown in Figure 3, the sampling location for the incremental layer of the direction of the three different positions, in order to later take the average value of the three tensile experiments in which One curve is shown in Figure 4.

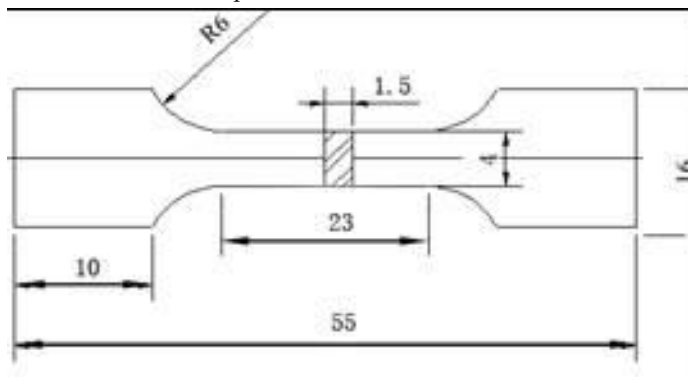


Figure 3: The dimensions of tensile samples



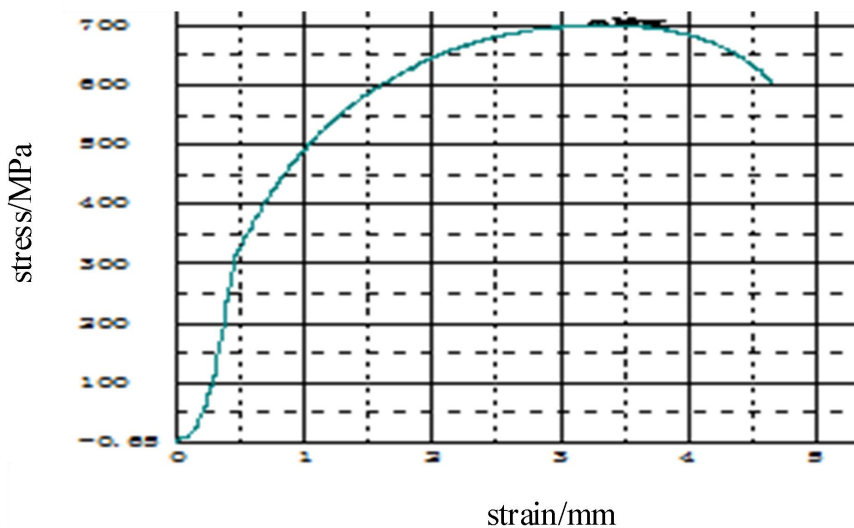


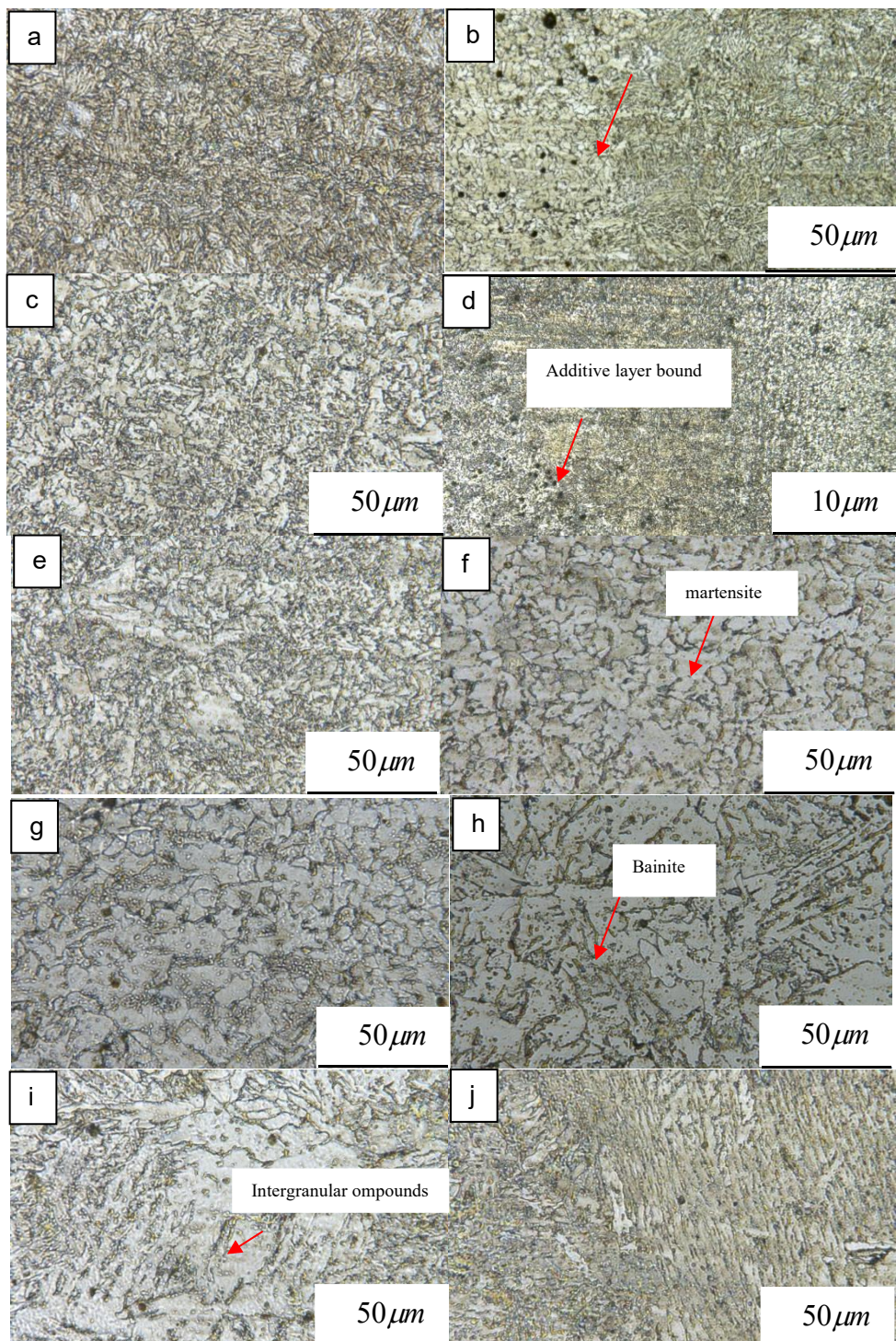
Figure 4: Tensile stress-stroke curve of sedimentary layer

Analysis of the experimental results show that the tensile strength along the augmentation heightening way on the tensile strength of 704.3MPa  $[(721.2+692.5+700.3)/3]$  or so, are not obvious yield strength, the conditional yield limit of about 412.4  $[(441.2+400.4+395.6)/3]$  MPa or so, higher than the yield strength of the annealed state rolled Cr12MoV substrate 210 MPa, and the elongation reaches 11.9%  $[(13.5+10.4+11.9)/3]$ , indicating that the 3D additive interlayer bonding strength is high and the interlayer plasticity is good.

### 3 Observation of micro-metallographic organisation

The multi-channel multilayer vertical walled parts were sampled for metallographic observation after the arc 3D additive. The metallographic specimens were prepared as follows: firstly, the specimens were cut with a wire cutter with a cutting size of  $16\text{mm}\times 16\text{mm}\times 6\text{mm}$ , and then polished with different grits of sandpaper after being smoothed on a SIST-200 grinder, and then polished with a diamond polishing agent with a grit size of 2  $\mu\text{m}$  on a MP-2A metallographic specimen polisher without any scratches; and then corroded with aqua regia (HCL:HNO<sub>3</sub>=1:3) on the specimens, and cleaned with wine and blown dry for microstructure observation and analysis. The specimen was corroded with aqua regia (HCL:HNO<sub>3</sub>=1:3), cleaned with wine, blown dry, and then observed and analysed the morphology of microstructure.

As shown in Figure 5, the matrix organisation is dense (shown in 5 (a)), with a clear fusion line between the bottom layer and the matrix, and fine grains (shown in 5 (b)), which benefited from the good heat dissipation conditions of the bottom layer at the initial stage of forming. The trend of heat dissipation conditions in the initial layers is gentle, with little change in grain size from layer to layer (shown in 5(c) (d)); up to the intermediate layer are isometric crystals, except that the grains after the intermediate layer are coarser than those in the matrix and initial layers (shown in 5(g) (h)); the outermost and second outermost layers can be seen as clearly orientated columnar crystalline organisation (shown in 5(i) (j)), due to the accumulation of heat from layer to layer in the process of metal deposition and the directional This is due to the accumulation of heat in the layers during the metal deposition process and the formation of directional heat dissipation conditions, resulting in the generation of coarse columnar crystalline tissue with directionality.



(a) Matrix; (b) Matrix on left, additive layer on right; (c) (d) Between additive layers; (e) First layer; (f) Second layer; (g) Intermediate layer; (h) Sub-intermediate layer; (i) Sub-outer layer; (j) Outer layer

Figure 5: Scanning image of typical layers

## 4 Wear test

Wear test specimen preparation: the use of wire cutting, along the height of the additive layer to intercept a



pair of specimens, the test parameters are shown in Table 2.

*Table 2 Wear testing parameters*

Friction parameters	Rotational speed (m/s)	payload (N)	Test duration (min)	counterpart	Friction method	Ambient temperature/humidity
Parameter value	1.09	30	60	Si <sub>3</sub> N <sub>4</sub> disc	Rotational motion with dry friction	24°C/65%RH

The coefficient of kinetic friction measured in this specimen is calculated according to the following formula:

$$\eta = \frac{9.45B}{10(A + C) - 2.5B} \quad (1)$$

where; is the equilibrium load derived from the experiment; is the applied load.

The test results are shown in Figure 6. The friction coefficient increases linearly and rapidly with time delay, from 0.107 to 0.271, and stabilised at 0.359, this is because at the beginning of the test, the surface of the specimen after grinding and processing there is always a certain degree of roughness, there are only a few profile peaks in contact at the beginning, so the friction coefficient rises faster, and the later contact surface is smooth to enter into a steady state, and the friction coefficient basically remains unchanged at the smaller value, which indicates that the additive layer has good abrasion resistance.

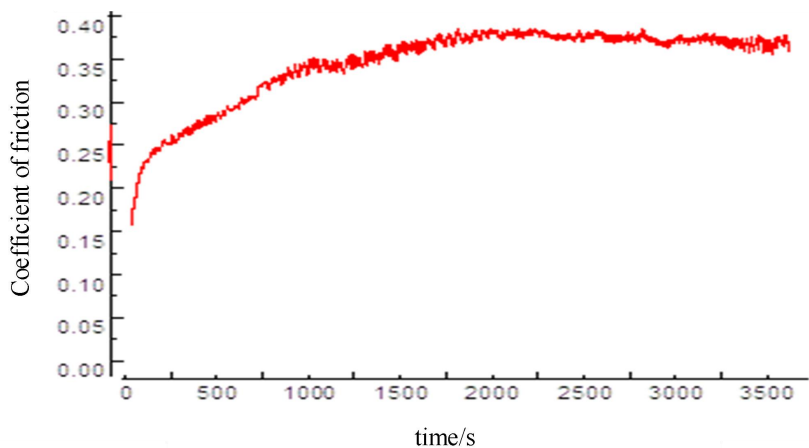


*Figure 6: Friction coefficient*

Figure 7 shows the results of specimen ESEM experiment. The observed pictures show that there are relatively obvious scratches and surface material flaking on the wear surface, and a large number of white abrasive chips are gathered in the local tissues, and the wear is a mixed mechanism of abrasive grain wear and adhesive wear. This is due to the block shedding and furrowing that occurs in the later stages of wear. The uneven distribution of stresses during the wear process results in the rupture, shedding and aggregation of hard phases, and the formation of furrows as these hard phases move relative to each other in the direction of friction on the soft substrate under the action of inertial forces. For carbon steel materials, the content, type, morphology, and distribution of alloying compounds and carbides Cm have a great influence on the wear

resistance of steel [6-12]. This melting material is rich in V, Cr, Mn for strong carbide formation elements, can promote the formation of carbide hard phase, these hard phase diffuse distribution in the matrix grain boundaries, play the role of nail rolling dislocations, strengthen the role of the matrix, which improves the microhardness of the additive layer, play a wear-resistant skeleton to improve the role of wear resistance in the abrasion test and service imperial process.

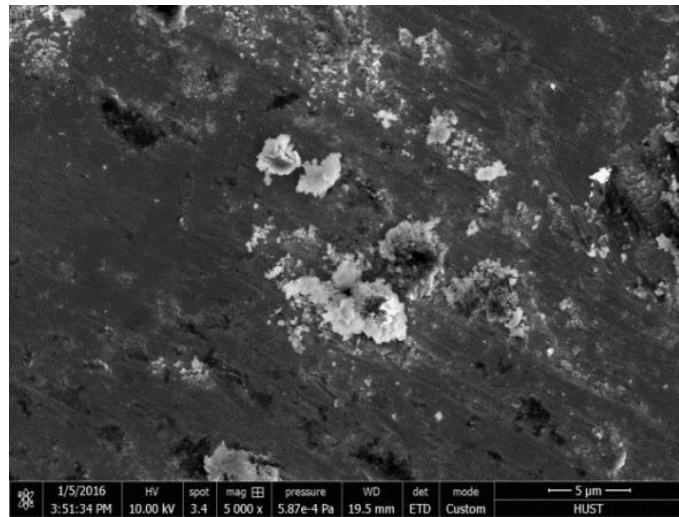


Figure 7: ESEM of Wear surface

## 5 Conclusion

- 1) H13 mould steel with self-medicated cored wire additive layer forming macro section without porosity, unfused and slag and other defects, and cold work mould steel Cr12MoV base material combination is good, the additive layer along the layer height direction microhardness, mechanical properties of high, weld state wear resistance is good;
- 2) Self-pharmaceutical cored wire for the ideal additive manufacturing wire and mould repair materials;
- 3) Arc fusion wire additive manufacturing technology provides an effective technical way for the green manufacturing and repair of metal parts.

## Funding

Huber Polytechnic University Research Project ( 24xjz01Y ) ; Innovation and Entrepreneurship Training Programme for University Students ( 20241092000F )

## REFERENCES

- [1] YU Hongmei, LIU Haiqiong, ZHOU Hongmei, et al. Research on Applications of Remanufacturing Technology for Die Steel Repair[J]. Electric Welding Machine, 2014, 44(11): 150-153.
- [2] WANG Shijie, WANG Haidong, LUO Feng. Research Status of Metal Additive Manufacturing Technology Based on Arc[J]. MW Metal Forming, 2018(1): 19-22.
- [3] XIONG Jun, XUE Yonggang, CHEN Hui, et al. Status and Development Prospects of Forming Control Technology in Arc-based Additive Manufacturing[J]. Electric Welding Machine, 2015, 45(9): 45-50.
- [4] YANG Xiaoyu, LI Yan, ZHAO Pengkang, et al. Research Status and Challenges of Wire and Arc



---

---

Additive Manufacturing in Material Preparation[J]. *Welding & Joining*, 2018(8): 14-20.

[5] GENG Haibin, XIONG Jiangtao, HUANG Dan, et al. Research Status and Trends of Wire and Arc Additive Manufacturing Technology[J]. *Welding & Joining*, 2015(11): 17-21.

[6] XU Yunchao, CAO Renqiu, SHUI Li. Effect of Bi on Microstructure and Frictional Wear Properties of Al-20%Si Alloy[J]. *Foundry*, 2017, 66(6): 622-625.

[7] ZHAN Qiang, LIANG Yihui, DING Jialuo, et al. A Wire Deflection Detection Method Based on Image Processing in Wire + Arc Additive Manufacturing[J]. *The International Journal of Advanced Manufacturing Technology*, 2017, 89(1): 755-763.

[9] DENG Yu, YU Shengfu, QIU Hongbin, et al. Study on Microstructure and Properties for a New Kind of Arc Sprayed Martensitic Stainless Steel Wear Resistance Coatings[J]. *Petro-Chemical Equipment*, 2012, 41(4): 6-9.

[10] XIA Ranfei. Study on Forming Dimensions and Process Parameters Optimization of Wire Arc Additive Manufacturing[D]. Wuhan: Huazhong University of Science and Technology, 2016.

[11] HE Bo, CHU Shasha, ZHANG Hongyu, et al. Laser Forming Properties of Cobalt Base Superalloy[J]. *Chinese Journal of Rare Metals*, 2017, 41(4): 350-355.

[12] JI Ying ping, WU Su jun, XU Liu jie, et al. Effect of Carbon Contents on Dry Sliding Wear Behavior of High Vanadium High Speed Steel[J]. *Wear*, 2012, 294: 239-245.